INDUCTIVE ENERGY STORAGE ELEMENTS BUILT AROUND FULLY CONTROLLABLE GAS-DISCHARGE DEVICES AND THEIR APPLICATION

V.D. Bochkov, N.M. Vereshchagin, F.G. Goryunov, V.A. Krestov, M.I. Lomaev, V.B. Merkulov, V.F. Tarasenko, and V.N. Shalygin

Scientific-Research Institute of Gas-Discharge Devices, Ryazan'
Institute of High-Current Electronics,
Siberian Branch of the Russian Academy of Sciences, Tomsk
Received August 1, 1995

Circuit schematics and results of testing of inductive energy storage elements built around fully controllable gas-discharge devices (FCGDs) have been presented. The following utmost parameters of voltage pulses have been obtained: pulse amplitude up to 100 kV *and pulse repetition frequency up to* 2 kHz. *The full control has been established over the FCGD drawing current up to* 500 A. *A nitrogen laser has been demonstrated to operate with efficiency of* 0.2% *of pump power when pumped by the inductive storage element.*

INTRODUCTION

Inductive storage elements constantly attract the attention of investigators[1-3] since they allow the power transferred to a load to be increased and the overall dimensions of a pump to be decreased. However, practical implementation of pumps with inductive energy storage is limited, especially in commercial devices intended for switching of current pulses of about 1 kA and higher at pulse repetition frequencies 10^2-10^3 Hz that can carry voltage pulses of several tens or hundreds of kilovolts when a circuit is switched. Fully controllable gas-discharge devices (FCGDs) show considerable promise as means for switching of current in pumps with inductive energy storage.

In 1937, Dryvesteyn[4,5] first reported on the creation of gas-discharge devices with bilateral control of anode current, i.e., on-off switches. In the 50s, these devices contained all main elements included in the design of their modern fully controllable gas-discharge analog - tasitron[6-8] (a fine-mesh control grid, an accumulating cathode, and hydrogen filling). It should be noted that tasitrons are not widely used in electronics and are now employed only in Russia (at the Scientific-Research Institute of Gas-Discharge Devices in Ryazan') for small-batch production. In addition to tasitrons, two high-power (delivering a pulse power of more than 100 kW) commercial devices should be mentioned intended to switch the load current when a control pulse is applied. They are vacuum switches (modulators built around pulsed lamps, electrooptic isolators, and transfer pentodes) and high-power transistors.

The main disadvantage of the vacuum switches is their low efficiency due to a high voltage drop across a vacuum gap. This energy characteristic is especially important when currents of the order of several tens of amperes and even higher are switched. Large energy losses call for the increase of overall dimensions of the device, increased consumption of cooling agents, and complicated power supply and cooling systems resulting in lower reliability of the equipment. Comparatively low rates of the current increase and decrease as well as low working voltage in comparison with gas-discharge and vacuum devices are typical for transistors.

In addition to these commercial devices, there are unique switches employed in electrophysical equipment, for example, explosively actuated wire switches and plasma opening switches.[1,2,9] Kotov et al.[3] reported the advent of opening switches based on commercial high-voltage semiconductor diodes.

This paper presents results of experimental study of inductive energy storage elements employing new fully controllable gas-discharge device with a cold anode for current switching as well as describes the use of a generator with inductive energy storage for pumping of a nitrogen laser.

FULLY CONTROLLABLE GAS-DISCHARGE DEVICES

At present there are several types of fully controllable gas-discharge devices. They are tasitrons[6-8,13] as well as superdense glow-discharge devices controlled by an external magnetic field[10,11] or by electric pulses applied to a fine-mesh grid as in tasitron.[1,12] Among drawbacks of tasitrons are a heated cathode and relatively low switched currents and working voltages. For example, highest-power tasitron TGU1-1000/25 develops a peak voltage of 25 kV and its switched current is no higher than 50 A (see Ref. 13). The devices controlled by the external magnetic field consume much power in a control circuit (up to 50% of the total switched power) and have long recovery time. The superdense glow-discharge devices controlled by electric signals are most promising for commercial production. A crossatron modulation switch (CMS) is one of the modifications of these devices. The crossatron is filled with hydrogen or helium at low pressure. A gas discharge in crossed electric and magnetic fields, with magnetic field created by permanent magnets and localized near the cathode, is a source of charged particles. At present the Hughes Research Laboratory (USA) advertises four models of crossatrons[14] delivering 20, 40, and 50 kV with an average current of 3 A that can switch currents up to 1 kA.

The FCGD produced by the Scientific-Research Institute of Gas-Discharge Devices and used in our investigations was capable of generating overvoltage pulses up to 100 kV. The FCGD differs from the crossatron[15] by more efficient screening of a high-voltage anode-grid chamber from cathode sputtering products. In addition, the main advantages of the crossatron - low discharge voltage drop and good controllability - are kept.

The tasitron, crossatron, and FCGD are controlled with a fine-mesh grid having 0.3-mm perforations. The anode current is switched in the following way. In the conduction mode (after switching of the device when current passes through it), a plasma is generated in the gap between the anode and cathode. If the voltage applied to the grid placed between the cathode and anode is lower than the plasma potential, the ion current will flow to the grid and the local potential difference will be produced resulting in secondary ionization compensating for the grid loss of ions. According to the data of probing reported in Ref. 16, the average electron temperature in this region is 42000-45000 K, i.e., there are a lot of electrons whose energies exceed the ionization potential. The grid potential may become much lower (by several tens of volts) than the plasma potential even without application of negative voltage due to the increase of the discharge current (several tens of amperes and higher) resulting in the increase of the plasma concentration. In Ref. 16 the grid potential differed from the plasma potential by 26-30 V. This initiates dense ion shells round the grid. The shell size (ΔX) is determined by the current density (J_i), ion mass (M_i), and potential difference (V) between the control grid and plasma. The relation among these parameters was derived within the Child-Langmuir theory of shells. It is given by the formula

$$J_i = 4/9\varepsilon_0(2e/M_i)^{1/2}\, V^{3/2}/(\Delta X)^2, \qquad (1)$$

where ε_0 is the permittivity of a vacuum and e is the electronic charge.

At working pressure typical of thyratrons (0.2-0.6 Torr) the shell size is small in comparison with the grid perforations. This leads to screening of the control electrode field and a loss of grid control. In the tasitron, crossatron, and FCGD the ion shell size is increased at lower pressure of the working gas (0.05-0.1 Torr) and ΔX increases further when a negative pulse is applied to the grid having small mesh size (0.32 mm) resulting in joining of ion shells of each mesh and anode electron current cutoff. The ion charge remaining in the anode-grid space moves to the grid, i. e., the anode current takes the path through the grid and vanishes without ionization of filling gas.

EXPERIMENTAL EQUIPMENT AND PROCEDURE

In our experiment, we tested several FCGDs at the Scientific-Research Institute of Gas-Discharge Devices (Ryazan') and at the Institute of High-Current Electronics of the Siberian Branch of the Russian Academy of Sciences (Tomsk). All FCGD were developed at the SRI GDD in Ryazan'. We performed the experiments with control circuits employing an additional thyratron built in the FCGD as an intrinsic quencher as well as an external thyratron generating a quenching signal.

Figure 1 shows the circuit schematic of FCGD switching with the intrinsic quencher. A pulsed magnetic field with a peak voltage of 30 mT was created by the induction coil L_m when the T2-12 thyristor was fired. In a series of experiments, we used a permanent magnetic field created by permanent samarium-cobalt magnets arranged along the side surface of the crossatron adjacent to its cathode. The T2-12 thyristor and the control thyratrons T_1-T_3 were triggered with controlled delays by the GI-1 pulse generator. The supply voltage on induction coil magnets U_m did not exceed 350 V, the voltage on capacitors of control and auxiliary discharge channels U_1 was about 1.7 kV, and the quenching voltage U_q varied between 0 and 4 kV. The inductance of the FCGD discharge circuit without the lumped inductance L_0 did not exceed 0.4 μH.

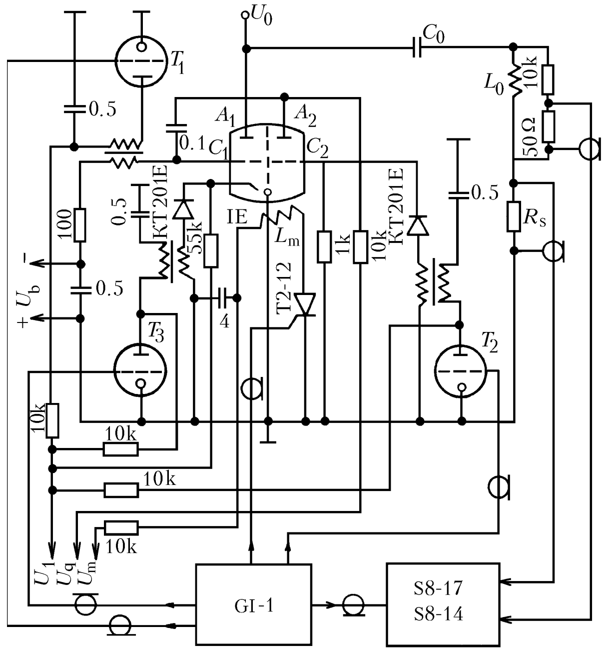

FIG. 1. Circuit schematic of a setup with a quencher built in the FCGD. Here T_1, T_2, and T_3 are the thyratrons, U_b is the bias voltage, C_0 is the accumulating capacitor, L_0 is the inductor of a discharge circuit, and IE is the initiation electrode.

The thyratron TGI1-60/5 was used in the circuit with external quencher. Figure 2 shows the circuit schematic illustrating the connection of the quenching thyratron. Here, U_q varied between 0 and 4 kV. To decrease the quenching signal generation time and to improve the switching characteristics of the TGI1-60/5 thyratron, its discharge circuit inductance was minimized and the supply voltages of the cathode heat and hydrogen generator circuits were specially adjusted. This allowed us to obtain the leading front width of a current pulse in a quenching channel no more than 20 ns.

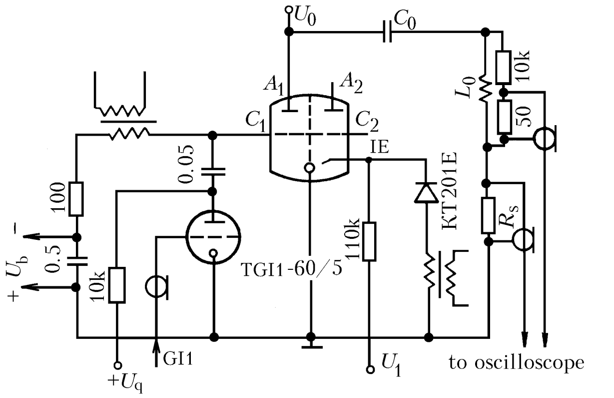

FIG. 2. Circuit schematics with external quenching thyratron.

Current shunts and voltage dividers built around the low-inductive TVO resistors, whose output signals were fed in the S8-14 or S8-17 oscilloscopes, were used to record current pulses.

CHARACTERISTICS OF GENERATORS WITH INDUCTIVE ENERGY STORAGE

Stable operation of generators was realized not only with the intrinsic quencher but also with the external thyratron generating a quenching signal. Stable current switching was obtained at anode voltages of power supply unit varying between 2 and 12 kV with a peak switching current of 0.5 kA. Maximum current switching rates $\mathrm{d}I/\mathrm{d}t$ of about 10^9 A/s were obtained with the external quenching thyratron. Switching time was as much as 110 ns. The generator operated stably in the periodic-pulse regime at pulse repetition frequencies up to 2 kHz and switching currents 150-200 A. Its peak output voltage was 100 kV with inductance L_0 of about 100 μH. Figure 3 shows oscillograms of the total current passing through the FCGD *(a)*, of the voltage on the inductor U_L for long *(b)* and short *(c)* sweeps obtained for different delays of a quenching pulse generated by the external thyratron. We note that maximum switching rates of currents passing through the FCGD were obtained when a quenching pulse was applied before the current reached its maximum, i. e., in the leading front of a current pulse (see Fig. 3).

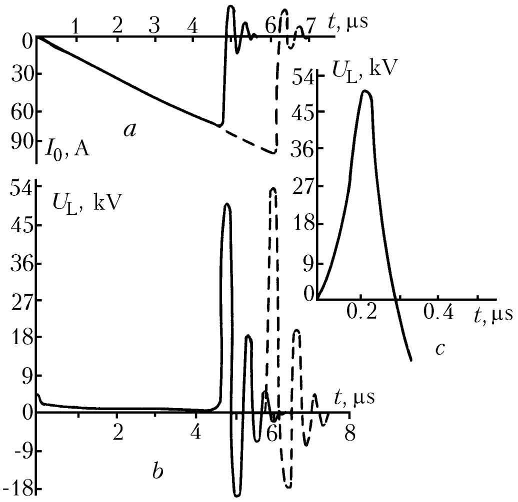

FIG. 3. Oscillograms of currents passing through the anode A_1 and voltage across the inductor U_L with external quenching thyratron. Here U_0=3.8 kV, f=200 Hz, and average current I_{av}=0.1 A.

SIMULATION OF THE OPERATION OF A GENERATOR WITH INDUCTIVE ENERGY STORAGE

To simulate the operation of a generator with inductive energy storage, we developed a program for designing a simplest discharge circuit shown in Fig. 4. Here, L_0 and C_0 may vary within wide limits and the FCGD resistance was taken equal to 0.5 Ω considering the results obtained by Baranov et al.[17] The temporal behavior of the FCGD resistance R_s and of the load resistance R_l was described by the following formulae:

$$R_s = \begin{cases} 0.5\ \Omega; & 0 \le t < t_1, \\ \mathrm{d}R/\mathrm{d}t(t - t_1) + 0.5; & t \ge t_1, \end{cases} \tag{2}$$

where t_1 denotes the start of current switching in the circuit and $\mathrm{d}R/\mathrm{d}t \sim 5\cdot 10^8$ Ω/s,

$$R_L = \begin{cases} 10^6; & 0 \le t < t_2, \\ 20 + 10^6/\exp[\alpha(t - t_2)]; & t \ge t_2, \end{cases} \tag{3}$$

where t_2 denotes the time of gas-discharge load breakdown at which the voltage across it reaches its breakdown threshold and $\alpha=2.3\cdot 10^8$ s^{-1}.

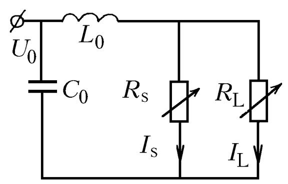

FIG. 4. Simplified circuit schematic of a generator with an inductive energy storage element. Here C_0 is the accumulating capacitor, L_0 is the inductor, R_s is the resistance of the current switch, R_L is the load resistance, I_s is the current passing through the switch, and I_L is the current passing through the load.

The values of α and dR/dt were adjusted by way of comparison of the design and experimental parameters when the generator operated with and without the load. Figure 5 shows design oscillograms of current passing through the FCGD I_s, current passing through the load I_L, and voltage across the load U_L. For a charging voltage of 2 kV with C_0=2 μF and L_0=30 μH, 70% of total current was switched to the load and the voltage across it reached about 28 kV. Our preliminary design revealed the dependence of ohmic losses in the FCGD on the load resistance when current was switched. To decrease power losses in the FCGD, the fast decrease and increase of the conductances of the FCGD and the load are desirable.

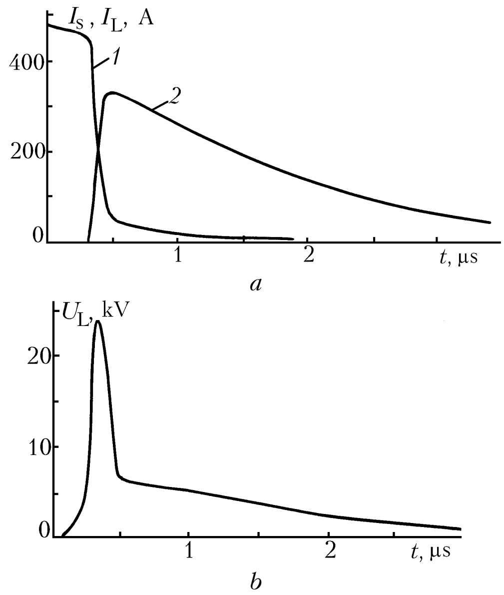

FIG. 5. Design oscillograms of currents passing through the switch I_s (1) and load I_L (2) and of the voltage across the load U_L.

A NITROGEN LASER PUMPED BY AN INDUCTIVE ENERGY STORAGE ELEMENT

One of the series of generators with inductive energy storage developed by us was used for pumping of a nitrogen longitudinal-discharge laser. A gas-discharge tube was 100 mm long and 6.6 mm in diameter. It was put in parallel with the FCGD. A laser cavity was formed by an aluminum-coated mirror and a parallel-sided quartz-crystal plate. Amplitude and shape of lasing pulses were measured with the FEK-22SPU photodiode and average output power was measured with the IMO-2N calorimeter. We performed measurements of single and periodic laser pulses with pulse repetition frequencies up to 10 Hz. In these experiments C_0=2 μF, L_0=32 μH, and discharge voltage U_0=2 kV.

Figure 6 shows oscillograms of voltage pulses on the inductor U_L corresponding to that applied to a laser chamber and of a lasing pulse at λ=337 nm. The laser emitted a radiation pulse in the leading front of a current pulse. The laser pulse width was about 7 ns FWHM, which is typical of the N^{2+} laser (system of bands $C^3\Pi_u$-$B^3\Pi_g$). Lasing efficiency was about 0.2% of pump energy per pulse. It is rather high for a nitrogen longitudinal-discharge laser. To obtain high total efficiency of gas lasers pumped by generators with inductive energy storage, one must match widths and shapes of pump and lasing pulses.[9] When the laser operated in the periodic-pulsed regime, the optimal output energy dependence was obtained at P=30 Torr with a charge voltage on the accumulating capacitor of only 2 kV.

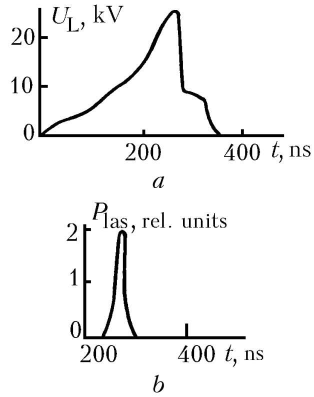

FIG. 6. Oscillograms of voltage pulses on the inductor L_0 and of a nitrogen laser pulse at λ=337 nm.

CONCLUSION

The results of experimental investigation of inductive energy storage elements built around fully controllable gas-discharge devices have been presented in the paper. We have obtained voltage pulses as high as 100 kV at pulse repetition frequencies up to 2 kHz and established full control of currents up to 500 A. A nitrogen laser pumped by the inductive storage element has been demonstrated to operate with the efficiency of about 0.2% of pump energy per pulse.

Applications of generators with inductive energy storage and switches - the FCGD - are highly diversified. They can be used in ozonizers, electrofilters harnessing pulsed nano- and microsecond streamer coronary discharges, laser systems, water purification systems, and so on. In addition, the FCGD can be used as modulators with complete or partial discharge of a capacitor, as charge-protection elements of various radio-electronic devices, and so on. It also should be noted that the FCGD can be used as a device with a cold cathode in the regime of complete discharge of the inductive storage element through it. We tested the FCGD in this regime and obtained that its lifetime exceeded 1000 h for a charging voltage of 25 kV, a peak current of 5 kA, and a pulse width of 1 μs at a pulse repetition frequency of 100 Hz.

REFERENCES

1. A. Quenther, M. Kristiansen, and T. Martin, *Opening Switches* (Plenum Press, New York and London), Vol. 1.

2. V.V. Kremnev and G.A. Mesyats, *Methods for Pulse Multiplication and Transform in High-Current Electronics* (Nauka, Novosibirsk, 1987), 226 pp.

3. Yu.A. Kotov, G.A. Mesyats, S.N. Rukin, and A.L. Filatov, Dokl. Ross. Akad. Nauk **333**, No. 3, 315 (1993).

4. M.J. Dryvesteyn, Germany Patent No. 674 321 (12 March 1937).

5. M.J. Dryvesteyn, Physica **4**, No. 8, 669 (1937).

6. E.O. Johnson, G. Olmsted, and W.M. Malter, Proc. IRE, 1350 (1954).

7. W. Espe and A. Hix, Feinwerktechnik **70**, 5 (1966).

8. A. Hix, Czechoslovakia Patent No. 90968 (15 July 1959).

9. A.N. Panchenko and V.F. Tarasenko, Kvant. Elektron. **17**, No. 1, 32 (1990).

10. R.J. Harvey and M.A. Lutz, IEEE Trans. Plasma Sci. **PS-4**, 210 (1976).

11. A.M. Arsh, V.D. Bochkov, V.P. Pyadin, et al., Inventor's Certificate No. 1593497 (1989).

12. A.I. Baranov and V.D. Bochkov, Prib. Tekhn. Eksp., No. 5, 209 (1991).

13. V.D. Dvornikov, S.T. Latushkin, L.M. Tikhomirov, et al., Prib. Tekhn. Eksp., No. 4, 108 (1972).

14. Laser Focus World **29**, No. 4, 75 (1993).

15. A.I. Baranov, A.M. Arsh, V.P. Pyadin, et al., Inventor's Certificate No. 1732391 (1992).

16. I.A. Zaitsev, I.G. Kozhevnikov, A.A. Nikolaev, and S.P. Shumakov, Elektr. Tekhn., No. 3, 33 (1969).

17. A.I. Baranov, K.V. Gurkov, M.I. Lomaev, et al., Prib. Tekhn. Eksp., No. 4, 108 (1994).